

# Contrast Interferometry using Bose-Einstein Condensates to Measure $h/m$ and $\alpha$

S. Gupta, K. Dieckmann, Z. Hadzibabic and D. E. Pritchard

Department of Physics, MIT-Harvard Center for Ultracold Atoms, and Research Laboratory of Electronics,  
MIT, Cambridge, MA 02139  
(December 2, 2024)

The kinetic energy of an atom recoiling due to absorption of a photon was measured as a frequency using an interferometric technique called “contrast interferometry”. Optical standing wave pulses were used as atom-optical elements to create a symmetric three-path interferometer with a Bose-Einstein condensate. The recoil phase accumulated in different paths was measured using a single-shot detection technique. The scheme allows for additional photon recoils within the interferometer and its symmetry suppresses several random and systematic errors including those from vibrations and ac Stark shifts. We have made a 15 ppm determination of the photon recoil frequency of sodium, using a simple realization of this scheme. Plausible extensions should yield a high precision ( $\approx 1$  ppb) measurement, allowing a ppb-level determination of  $h/m$  and the fine structure constant  $\alpha$ .

PACS numbers: 39.20.+q, 3.75.Dg, 6.20.Jr, 3.75.Fi

Accurate measurements of the fine structure constant  $\alpha$  in different subfields of physics, like atomic physics, QED and condensed matter physics, offer one of the few checks for global errors across the different subfields. The measurement of  $(g-2)$  for the electron and positron at 4 ppb [1,2] has stood as the best  $\alpha$  measurement for fifteen years. The second most accurate value of  $\alpha$ , at 24 ppb comes from condensed matter experiments [3]. This is worse by a factor of six, limiting the scientific value of cross-field comparisons. A new and more robust route based on atomic physics measurements has emerged in the last decade [4]:

$$\alpha^2 = \left( \frac{e^2}{\hbar c} \right)^2 = \frac{2R_\infty}{c} \frac{h}{m_e} = \frac{2R_\infty}{c} \frac{m_p}{m_e} \frac{M}{M_p} \frac{h}{m} . \quad (1)$$

The Rydberg constant  $R_\infty$  is known to 0.008 ppb [5,6] and the proton-electron mass ratio  $m_p/m_e$  to 2 ppb [7].  $M_p$  is the mass of the proton in atomic units, and  $M$  and  $m$  are the mass of some test particle in atomic and SI units respectively. Eq. 1 offers the possibility of a measurement of  $\alpha$  at the ppb level if  $M$  and  $h/m$  can be determined accurately.

$h/m$  can be measured by comparing the deBroglie wavelength and velocity of a particle, as demonstrated by Krüger, whose measurement using neutrons has yielded a value for  $h/m_n$  accurate at 73 ppb [8]. For an atom,  $h/m$  can be extracted from a measurement of the photon recoil frequency

$$\omega_{\text{rec}} = \frac{1}{2} \frac{\hbar}{m} k^2 , \quad (2)$$

where  $k$  is the wavevector of the photon absorbed by the atom. Recent experiments allow Eqs. 1 and 2 to be applied to cesium.  $M_{\text{Cs}}$  is now known to 0.17 ppb [9] and  $k_{\text{Cs}}$  to 0.12 ppb [10].  $\omega_{\text{rec,Cs}}$  has been measured to high precision at Stanford [11–13] using an atom interferometer based on laser-cooled atoms. Similar experiments are possible with alkali atoms like sodium and rubidium

where  $M$  has been measured [9] and  $k$  is accurately accessible [10].

The Stanford scheme to measure  $\omega_{\text{rec}}$  uses different internal states to separately address different interferometer paths. An alternative interferometer to measure the photon recoil using laser cooled atoms in the same internal state was demonstrated using rubidium atoms [14], but seems unlikely to give competitive precision.

In this Letter, we report the development of a new type of atom interferometer which shows great promise for a high precision measurement of the photon recoil frequency. It extends the previous schemes and combines their advantages. Our scheme utilizes a symmetric three-path configuration which encodes the photon recoil phase in the *contrast* of the interference fringes, rather than in their *phase*. Because it is insensitive to the fringe phase, the method is not sensitive to vibrations, accelerations or rotations. The symmetry also suppresses errors from magnetic field gradients and our use of the same internal state suppresses errors from ac Stark shifts. A crucial aspect of this new interferometer is the use of atomic samples with sub-recoil momentum distribution. We use a Bose-Einstein condensate (BEC) as a bright atom source for this interferometer. This allows the contrast oscillations to persist for many cycles, permitting accurate determination of the recoil phase in a single experimental “shot” and allows for extra photon recoils to be added within the interferometer, which increases the recoil phase shift quadratically.

To explain the basic principle of our scheme, we first look at the asymmetric interferometer of Fig. 1(a). At time  $t = 0$  a BEC is split coherently into two momentum components,  $|2\hbar k\rangle$  and  $|0\hbar k\rangle$ , by a first order Bragg  $\pi/2$ -pulse [15]. These are shown as paths 1 and 2 in the figure. At time  $t = T$ , the application of a second order Bragg  $\pi$ -pulse reverses the direction of path 1, while leaving path 2 unaffected. Around  $t = 2T$ , a moving matter wave grating, with spatial periodicity  $\lambda/2$  (wavevector  $2k = \frac{2\pi}{\lambda/2}$ ), is formed due to the interference of the two

paths where they overlap. The phase of this grating at  $2T$  is determined by the relative phase  $\Phi_1 - \Phi_2 = 8\omega_{\text{rec}}T$ , accumulated between paths 1 and 2 due to the difference in their kinetic energies. A measurement of this phase for different values of  $T$  will then determine  $\omega_{\text{rec}}$ . If path 1 is accelerated by additional photon recoils to state  $|N2\hbar k\rangle$ , the corresponding grating phase will be  $\Phi_1 - \Phi_2 = N^2 8\omega_{\text{rec}}T$ , leading to an  $N^2$ -fold improvement in the  $\omega_{\text{rec}}$  measurement precision. The fringes of all atoms will be in phase at time  $t = 2T$ , forming a high-contrast matter wave grating. This dephases in a time  $\frac{1}{k\Delta v}$ , the coherence time, where  $\Delta v$  is the finite velocity spread of the initial cloud of atoms.

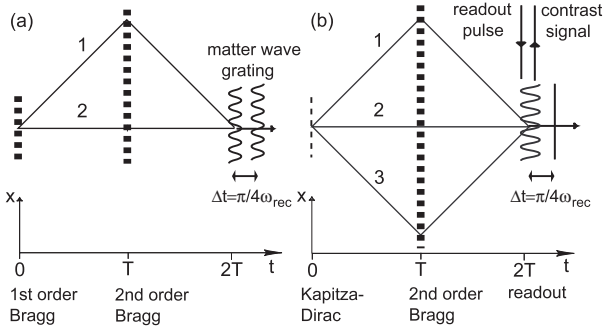


FIG. 1. Space-Time representation of the contrast interferometer. (a) shows a simple 2-path interferometer sensitive to the photon recoil phase. The matter wave grating at  $2k$  is shown at  $2T$  and at  $2T + \pi/4\omega_{\text{rec}}$ . The extension to the 3-path geometry is shown in (b). The overall  $2k$  grating has large contrast at  $2T$  and zero contrast at  $2T + \pi/4\omega_{\text{rec}}$ .

Extension of this interferometer to a symmetric three-path arrangement is shown in Fig. 1(b). Three momentum states (paths 1, 2 and 3) are generated by replacing the first Bragg pulse with a short Kapitza-Dirac pulse [15]. At  $t = 2T$ , there are now two matter wave gratings with period  $\lambda/2$ , one from paths 1 and 2 and one from paths 2 and 3. These move in opposite directions at a relative speed  $4\hbar k/m$ . If the maxima of the two gratings line up to produce large contrast at time  $t$ , the maxima of one will line up with the minima of the other at  $t + \pi/4\omega_{\text{rec}}$ , to produce zero contrast. This results in an oscillatory growth and decay of the contrast of the overall pattern with time. The recoil induced phase can be determined from this temporally oscillating contrast.

In our experiment, the time evolution of this contrast is monitored by continuously reflecting a weak probe beam from the grating in the backward direction (the additional matter wave grating formed by paths 1 and 3 has period  $\lambda/4$ , to which the 2-photon reflection is not sensitive). The reflected signal can be written as

$$\begin{aligned} S(T, t) &= C(T, t) \sin^2 \left( \frac{\Phi_1(t) + \Phi_3(t)}{2} - \Phi_2(t) \right) \\ &= C(T, t) \sin^2(8\omega_{\text{rec}}T + 4\omega_{\text{rec}}(t - 2T)), \end{aligned} \quad (3)$$

where  $C(T, t)$  is an envelope function whose width is the grating coherence time,  $\frac{1}{k\Delta v}$ . This motivated our use of a BEC atom source. This allowed many contrast oscillations in a single experimental shot. Using the phase of the reflection at  $t = 2T$ ,  $\Phi(T) = 8\omega_{\text{rec}}T$ , the recoil frequency can be determined by varying the time  $T$ . The symmetry of the three-path contrast scheme forces random errors such as vibrational phase shifts and systematics such as magnetic field gradients to cancel in the evaluation of  $\frac{\Phi_1(t) + \Phi_3(t)}{2} - \Phi_2(t)$ .

In this experiment, we have realized the interferometer of Fig. 1(b) and extracted a value for the photon recoil frequency of sodium to 15 ppm precision. We also show the insensitivity of the contrast signal to vibrational noise and the quadratic scaling of the recoil phase with  $N$ .

We used sodium BEC's containing a few million atoms in the  $|F = 1, m_F = -1\rangle$  state as our atom source. The light pulses were applied  $\approx 15$  ms after releasing the BEC from a weak magnetic trap. This lowered the peak density to about  $10^{13} \text{ cm}^{-3}$ , thus preventing superradiance effects [16] and reducing frequency shifts from mean field interactions. Two horizontal counterpropagating (to  $\leq 1$  mrad) laser beams were used for the diffraction gratings. The light for the gratings was red-detuned by 1.8 GHz from the sodium  $D_2$  line. Rapid switching ( $< 100$  ns) and intensity control of the light pulses was done by an acousto-optic modulator (AOM) common to the two beams. The phase and frequency of each beam were controlled by two additional AOMs, driven by two phase-locked frequency synthesizers.

The interferometer pulse sequence was started with a  $1\mu\text{s}$ , square Kapitza-Dirac pulse, centered at  $t = 0$ . We adjusted the beam intensity, to put  $\approx 25\%$  of the condensate in each of the  $|\pm 2\hbar k\rangle$  diffracted orders. This choice yielded the best final contrast signal. The second order Bragg pulse was centered at  $t = T$  and was close to Gaussian shaped with a width of  $7.6\mu\text{s}$ . The intensity was chosen to effect a  $\pi$ -pulse between the  $|\pm 2\hbar k\rangle$  states. The smooth pulse shape reduced the off-resonant population of undesired momentum states, yielding a transfer efficiency of  $> 90\%$ . The third pulse, used for reading out the contrast signal, was centered at  $t = 2T$  and was typically  $50\mu\text{s}$  long. One of the Bragg beams was used as the readout beam while the other was blocked.

The light reflected from the atoms was separated from the readout beam path using a beamsplitter and directed by an imaging lens onto a photomultiplier. A typical interferometer signal is shown in Fig. 2. We observed the expected contrast oscillations at frequency  $8\omega_{\text{rec}}$  corresponding to a  $5\mu\text{s}$  period for sodium. The contrast was  $\approx 60\%$  and the width of the envelope was  $\approx 30\mu\text{s}$ . We obtained the recoil phase  $\Phi(T)$  from the contrast signal by fitting the observed data to a sinusoidal function as in Eq. 3.

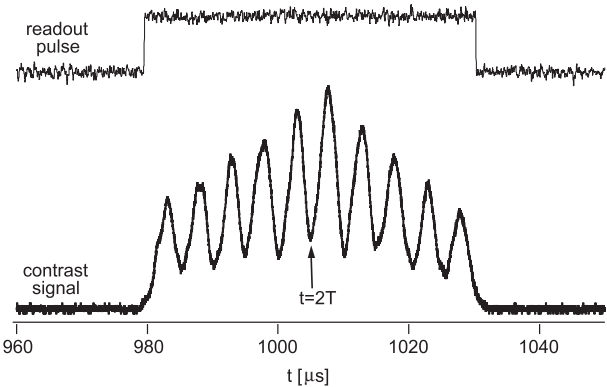


FIG. 2. Typical single-shot signal from the contrast interferometer.  $T = 502.5 \mu\text{s}$  for this example. Ten oscillations are observed during the  $50 \mu\text{s}$  readout. A low-pass filter at  $300 \text{ kHz}$  (12dB per octave) was applied to the signal.

The signal also contained a small pedestal of similar width as the envelope. This consists of a constant offset from residual background light and spontaneous emission from the atoms, and a smoothly varying contribution from a small asymmetry in the  $|2\hbar k\rangle$  and  $| - 2\hbar k\rangle$  amplitudes of  $< 5\%$ . This asymmetry creates a non oscillating component of the  $2k$  matter wave grating which decays with the same coherence time. The uncertainty of the fitted phase is about 10 mrad, even if we neglect the envelope function, and assume a constant amplitude extended over a few central fringes. Similar uncertainty was obtained for large interferometer times  $T \approx 3 \text{ ms}$ . We observe a shot-to-shot variation in the fitted value of the phase of about 200 mrad. We attribute this to pulse intensity fluctuations which randomly populated undesired momentum states at the  $< 10\%$  level. This resulted in spurious matter wave gratings which randomly shifted the observed recoil phase.

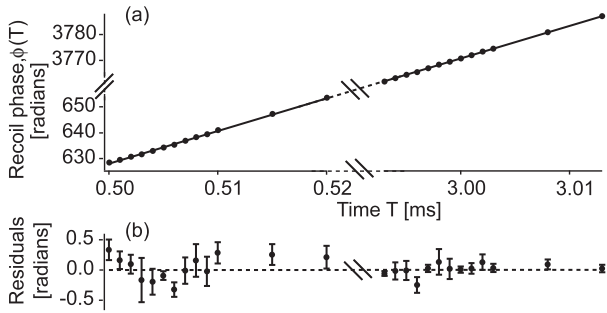


FIG. 3. Measurement of the photon recoil frequency in sodium. Two sets of recoil phase scans, around  $T = 0.5 \text{ ms}$  and around  $T = 3 \text{ ms}$ , are shown in (a). The slope of the linear fit gave the recoil frequency to 15 ppm. Each point is the average of five measurements. The error bars are assigned to be the standard deviation of the five measurements at each point and are shown together with the fit residuals in (b).

The recoil frequency was determined by measuring the recoil phase around  $T = 0.5 \text{ ms}$  and around  $T = 3 \text{ ms}$

(Fig. 3). The pulse intensities were adjusted between these two values to compensate for the atoms dropping along the vertical axis of the gaussian laser beam profile. An upper bound on  $T$  was set by the beam size of 2 mm, and the available laser power. A straight line fit to these data produced a value for the sodium photon recoil frequency  $\omega_{\text{rec},\text{Na}} = 2\pi \times 24.9973 \text{ kHz} (1 \pm 1.5 \times 10^{-5})$ . This is  $2 \times 10^{-4}$  lower than the sub-ppm value calculated using  $\lambda_{\text{Na}}$ ,  $m_{\text{Cs}}/m_{\text{Na}}$  and  $h/m_{\text{Cs}}$  [17,9,10,13]. The systematic shift from differential mean field interactions due to unequal populations in the three paths may explain this deviation. Estimated errors from beam misalignment and wavefront curvature have the same sign as the observed deviation but several times lower magnitude.

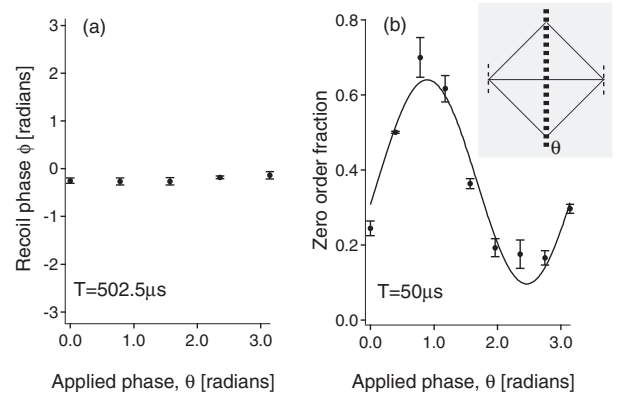


FIG. 4. Vibration insensitivity of the contrast interferometer. (a) shows the measured recoil phase at  $T = 502.5 \mu\text{s}$  from the contrast interferometer as a function of the applied phase  $\theta$  of the second pulse. The recoil phase is constant and demonstrates the insensitivity of the interferometer to phase noise of the gratings. (b) shows the fractional population of the  $|0\hbar k\rangle$  state from the phase-sensitive interferometer (inset) for a similar scan of  $\theta$  at  $T = 50 \mu\text{s}$ . Also shown is the best-fit sinusoid of the expected period. The oscillation demonstrates the phase sensitivity of any position-sensitive readout. The points and their error bars are evaluated as in Fig. 3.

To demonstrate the insensitivity of the measurement to phase noise of the light due to mirror vibrations, we intentionally varied the phase  $\theta$  of the second pulse relative to the first one [18]. The contrast signal is not affected by such phase variations, as shown in Fig. 4(a). We compared our contrast interferometer signal to a phase-sensitive readout method, shown in the inset of Fig. 4(b). This was realized by replacing the readout pulse with a third pulsed  $1 \mu\text{s}$  light grating in the Kapitza-Dirac regime. This pulse was phase-locked to the first two pulses and projected the phase of the  $2k$  pattern at  $t = 2T$  onto the fractional populations of the states  $|0\hbar k\rangle$ ,  $|2\hbar k\rangle$ , and  $| - 2\hbar k\rangle$  which leave this interferometer. The populations were measured by time-of-flight absorption imaging. The  $|0\hbar k\rangle$  fraction is shown for the same variation of  $\theta$ , in Fig. 4(b). The sinusoidal oscillation [19] clearly displays the phase sensitivity.

These two interferometers respond differently to mir-

rror vibrations. For large values of  $T$ , we have observed the effect of the mirror vibrations directly. At  $T \approx 3$  ms, the shot-to-shot fluctuations of the phase-sensitive interferometer was of the order of the expected fringe contrast. This is also in agreement with observations with a standard Mach-Zehnder interferometer constructed both by us and in [20]. In comparison, the stability of the contrast interferometer signal is independent of  $T$  within our measurements. This can be seen from the comparable statistical error bars for short and long times in Fig. 3(b). In fact, the residuals and the corresponding error bars are smaller at the longer times. We attribute this to the decreased amplitude of some of the spurious gratings at longer times, due to reduced overlap of the contributing wavepackets.

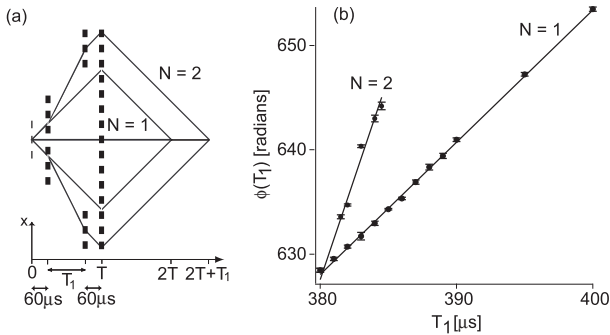


FIG. 5. Demonstration of the quadratic scaling of the recoil phase with additional Bragg pulses. (a) shows the  $N = 1$  (inner) and  $N = 2$  (outer) interferometers used. (b) shows the recoil phase at the recombination time under variation of  $T_1$ . The  $N = 1$  data set is the same as that in Fig. 3. The points and their error bars are evaluated as in Fig. 3.

The quadratic scaling of the accumulated recoil phase with the number of transferred recoils  $N$ , was demonstrated by comparing  $N = 1$  and  $N = 2$  interferometers. An  $N = 2$  geometry, shown in Fig. 5(a), was realized using two additional first order Bragg  $\pi$ -pulses spaced  $T_1$  apart. The acceleration pulse at  $t = 60\mu\text{s}$  drove transfers from  $|\pm 2\hbar k\rangle$  to  $|\pm 4\hbar k\rangle$ . The deceleration pulse at  $t = T_1 + 60\mu\text{s} = T - 60\mu\text{s}$  drove transfers from  $|\pm 4\hbar k\rangle$  to  $|\pm 2\hbar k\rangle$ . During the period  $T_1$ , the paths 1 and 3 accumulate phase  $2^2 = 4$  times faster in the  $N = 2$  scheme than in the  $N = 1$  scheme. Additional time  $T_1$  is required for the three paths to recombine in the  $N = 2$  scheme. For this geometry, the  $N = 2$  recoil phase should therefore evolve three times faster as a function of  $T_1$  than the  $N = 1$  recoil phase. The corresponding data sets are shown in Fig. 5(b). The linear fits give a slope ratio of  $3.06 \pm 0.1$ , in agreement with the expectation. At present, we do not have sufficient control over the timing and phase of the intermediate pulses to improve our  $N = 1$  measurement precision by using  $N > 1$ .

In conclusion, we have demonstrated a contrast interferometer which has several desirable features for a high accuracy measurement of the photon recoil fre-

quency. Such a measurement would involve converting to an atomic fountain setup with vertical Bragg beams. In this geometry,  $T$  can be extended by more than an order of magnitude. The order  $N$  of the interferometer can also be increased. Direct scaling of our current precision of 15 ppm yields 1 ppb for  $T = 100$  ms and  $N = 20$ . In addition, better control of interferometer pulses will reduce our statistical uncertainties arising from spurious matter wave gratings. Vibrations and ac Stark shifts have been of great concern in earlier precision measurement schemes [12]. Our demonstrated insensitivity to phase noise from mirror vibrations will greatly alleviate the need for vibration isolation of the system. Our scheme is insensitive to ac Stark shifts and to both magnetic bias field and gradient, even if they are time-dependent. This will relax magnetic shielding constraints. We hope to obtain a  $< 1$  ppb value for  $\omega_{\text{rec}}$  in a second generation experiment in which BECs are created elsewhere and transported into the interferometer [21].

We thank W. Ketterle for valuable discussions. This work was supported by the NSF, ONR, ARO, NASA and the David and Lucile Packard Foundation.

- [1] R. S. Van Dyck, Jr., P. B. Schwinberg, and H. G. Dehmelt, Phys. Rev. Lett. **59**, 26 (1987).
- [2] T. Kinoshita, Phys. Rev. Lett. **75**, 4728 (1995).
- [3] M. E. Cage et. al., IEEE Trans. Instr. Meas. **38**, 284 (1989).
- [4] B. Taylor, Metrologia **31**, 181 (1994).
- [5] C. Schwob et. al., Phys. Rev. Lett. **82**, 4960 (1999).
- [6] Th. Udem et. al., Phys. Rev. Lett. **79**, 2646 (1997).
- [7] D. L. Farnham, R. S. Van Dyck, Jr., and P. B. Schwinberg, Phys. Rev. Lett. **75**, 3598 (1995).
- [8] E. Krüger, W. Nistler, and W. Weirauch, Metrologia **35**, 203 (1998).
- [9] M. P. Bradley et. al., Phys. Rev. Lett. **83**, 4510 (1999).
- [10] Th. Udem, J. Reichert, R. Holzwarth, and T. W. Hänsch, Phys. Rev. Lett. **82**, 3568 (1999).
- [11] D. S. Weiss, B. C. Young, and S. Chu, Phys. Rev. Lett. **70**, 2706 (1993).
- [12] B. C. Young, Ph.D. thesis, Stanford (1997).
- [13] J. M. Hensley, Ph.D. thesis, Stanford (2001).
- [14] S. B. Cahn et. al., Phys. Rev. Lett. **79**, 784 (1997).
- [15] S. Gupta, A. E. Leanhardt, A. D. Cronin, and D. E. Pritchard, Cr. Acad. Sci. IV-Phys **2**, 479 (2001), and references therein.
- [16] S. Inouye et. al., Science **285**, 571 (1999).
- [17] P. Juncar, J. Pinard, J. Hamond, and A. Chartier, Metrologia **17**, 77 (1981).
- [18] We scanned  $\theta$  by electronically shifting the phase of the rf signal used to drive one of the two Bragg AOMs.
- [19] The division of population into three interferometer output ports caused the observed 74% ( $< 100\%$ ) contrast. We have observed  $\approx 100\%$  contrast in a standard Mach-Zehnder interferometer.
- [20] Y. Torii et. al., Phys. Rev. A. **61**, 041602 (2000).
- [21] T. L. Gustavson et. al., Phys. Rev. Lett. **88**, 020401 (2002).